

# Brittle dynamic fracture of crystalline cubic silicon carbide (3C-SiC) via molecular dynamics simulation

Hideaki Kikuchi

Department of Computer Science, Louisiana State University, Baton Rouge, Louisiana 70803-4020

Rajiv K. Kalia, Aiichiro Nakano, and Priya Vashishta

Collaboratory for Advanced Computing and Simulations, Department of Chemical Engineering & Materials Science, Department of Computer Science, and Department of Physics & Astronomy, University of Southern California, Los Angeles, California 90089-0242

Paulo S. Branicio

Departamento de Física, Universidade Federal de São Carlos, São Carlos, SP 13565-905, Brazil

Fuyuki Shimojo

Department of Physics, Kumamoto University, Kumamoto 860-8555, Japan

(Received 24 February 2005; accepted 13 October 2005; published online 29 November 2005)

Brittle fracture dynamics for three low-index crack surfaces, i.e., (110), (111), and (100), in crystalline cubic silicon carbide (3C-SiC) is studied using molecular dynamics simulation. The results exhibit significant orientation dependence: (110) fracture propagates in a cleavage manner; (111) fracture involves slip in the  $\{11\bar{1}\}$  planes; and crack branching is observed in (001) fracture. Calculated critical energy release rates, which characterize fracture toughness, are compared with available experimental and *ab initio* calculation data. © 2005 American Institute of Physics. [DOI: 10.1063/1.2135896]

## I. INTRODUCTION

Potential applications of silicon carbide (SiC) for electronic and structural devices have created strong interest in its physical and mechanical properties.<sup>1</sup> Due to the brittleness of SiC, there is a great need for understanding its fracture behaviors for structural applications. Dynamic fracture has been studied experimentally and by large-scale atomistic simulation in various materials.<sup>2-4</sup> However, it has been reported that molecular dynamics (MD) simulations with empirical interatomic potentials often fail to describe fracture in real materials even qualitatively.<sup>5</sup> For example, the widely used Stillinger-Weber potential had to be modified to realize a brittle fracture in silicon.<sup>6</sup> Recently, we have shown that MD simulations with our interatomic potential reproduce not only the known fracture behaviors for different crystallographic orientations but also experimental fracture toughness values in crystalline GaAs.<sup>7</sup> In this paper, we present MD simulations of brittle dynamic fracture in crystalline cubic silicon carbide (3C-SiC) using our interatomic potential. The results exhibit significant orientation dependence: (110) fracture is cleavage, whereas (111) and (001) fractures are unstable against slip and branching, respectively.

The interatomic potential used in this study has been validated by comparing a number of physical quantities with corresponding experimental data. The potential parameters are chosen to reproduce the lattice constant, the elastic constants ( $c_{11}$  and  $c_{12}$ ), and the cohesive energy of 3C-SiC crystal. Reasonable agreements between MD and experimental results are also obtained for: (i) high-pressure structural transformation in crystalline SiC including both forward and

reverse transformations;<sup>8</sup> (ii) phonon density of states of crystalline 3C-SiC; (iii) sintering temperature of nanophase SiC;<sup>9</sup> and (iv) amorphous structure.<sup>10</sup>

## II. MD SIMULATION

The strip geometry used in this study is shown schematically in Fig. 1. The top and bottom layers of the strip of width  $10 \text{ \AA}$  in the  $z$  direction are held rigidly during the entire simulation to apply strain to the system. The periodic boundary condition is applied in the  $y$  direction (with plane-strain condition), but the  $x$  and  $z$  directions have free surfaces. A thin notch of half the system length is inserted by removing atoms in the middle of the two fixed layers to initiate a crack in the  $x$  direction. The crack plane is parallel to the  $xy$  plane. This strip geometry facilitates simple calculation of the energy flux into the crack.<sup>11</sup> The energy to make continuous crack advance is provided by uniaxially stretching the system along the  $z$  direction in our MD simulations. In an initial MD run, the system is quenched to relax the free

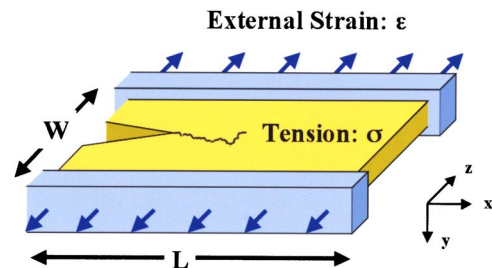


FIG. 1. Schematic of the system configuration used in fracture simulations. The strip geometry allows a simple calculation of the mechanical energy release rate,  $G$ .

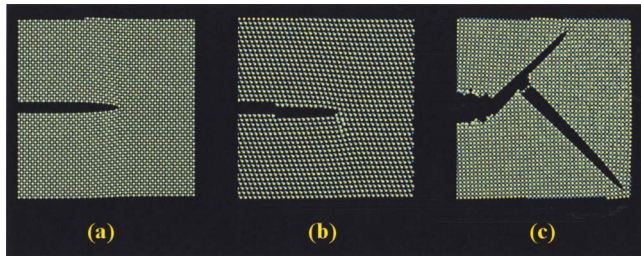


FIG. 2. Atomic configurations near the crack tips in brittle fracture of 3C-SiC. (a) shows (110) to be a cleavage surface; (b) shows that (111) is not a cleavage surface since dislocation emission deforms the crack tip; (c) shows that fracture along (001) surfaces is unstable to branching along {110} surfaces.

surfaces by scaling velocities of atoms. The system is then stretched gradually up to slightly below the critical strain,  $\varepsilon_c$ , which is predicted by Griffith's theory. To eliminate an artificial stress waves in stresses  $\sigma_{xx}$  and  $\sigma_{zz}$  due to the simulation schedule, the system is quenched again. To calculate crack-tip speeds at different strains, the system is subsequently stretched to a desired strain at a strain rate,  $\dot{\varepsilon}$ . The strain rate is  $\dot{\varepsilon}=10^{-6}\Delta t^{-1}$ , where  $\Delta t=1$  fs is the time step used in the simulations.

The mechanical energy release rate,  $G$ , in the strip geometry is the amount of energy, per unit area, that is supplied by the elastic energy stored in the system. It is calculated by integrating the stress-strain curve with respect to strain,  $\varepsilon$

$$G = W \int_0^{\varepsilon} d\varepsilon' \sigma(\varepsilon'),$$

where  $W$  is the strip width in the  $z$  direction (see Fig. 1) and  $\sigma$  is the  $zz$  component of the stress well ahead of the crack tip. At a strain above  $\varepsilon_c$ , crack propagation at constant velocity is achieved after an initial transient. The crack-tip speed is thus obtained for each value of  $G$ .

### III. RESULTS

MD simulations are carried out for three low-index crack surfaces: (110), (111), and (001). The system size and number of atoms for each system are  $616 \times 17 \times 185 \text{ \AA}^3$  and 190 000 atoms for (110) (the crack propagates in the  $[\bar{1}10]$  direction);  $641 \times 18 \times 181 \text{ \AA}^3$  and 200 000 atoms for (111)  $[\bar{1}\bar{1}2]$ ;  $610 \times 17 \times 192 \text{ \AA}^3$  and 190 000 atoms for (001)  $[100]$  fracture. While the initial temperature of the system is nearly zero, it increases as the crack advances. Temperature control, which may affect crack-tip dynamics, is not applied in this study. Nevertheless, the average temperature remains below 100 K during the entire simulation.

Figure 2(a) shows a snapshot of (110) brittle fracture at  $G=3.9 \text{ J/m}^2$ . In the (110) brittle fracture, the crack travels in a steady and cleavage manner along the  $x$  direction, and the crack tip is atomically sharp. Calculated critical energy release rate,  $G_c=3.5 \text{ J/m}^2$ , is slightly larger than  $2\gamma(110)=3.4 \text{ J/m}^2$ , where  $\gamma(110)$  is the (110) surface energy. The small difference between  $G_c$  and  $2\gamma$  may be attributed to lattice trapping in both (110) and (111) brittle fracture.

Lattice trapping is a manifestation of the atomistic discreteness of the crystalline lattice, and it causes the crack to

TABLE I. Fracture toughness  $T_c$ , critical energy release rate  $G_c$ , and surface energy  $\gamma$  of 3C-SiC (110), (111), and (001) surfaces. The present molecular dynamic (MD) results are compared with the other theoretical results.

	(110)	(111)	(001)
$T_c$ (MPa m <sup>1/2</sup> )	1.26	1.52	1.30
$G_c$ (J/m <sup>2</sup> )	3.5	4.6	5.1
$2\gamma$ (J/m <sup>2</sup> )—present	3.4	4.2 <sup>a</sup>	6.8 <sup>a</sup>
$2\gamma$ (J/m <sup>2</sup> )—other theories	3.1 <sup>b</sup> , <sup>c</sup> , 2.0 <sup>d</sup> , 3.6 <sup>e</sup>	2.5 (shuffle), 8.2 (glide) <sup>e</sup>	4.6 <sup>c</sup>

<sup>a</sup>Average surface energy of Si- and C-terminated ideal surfaces.,

<sup>b</sup>Reference 19.

<sup>c</sup>Reference 22.

<sup>d</sup>Reference 20.

<sup>e</sup>Reference 21.

remain stable and not to advance until the load reaches  $G_c$ , which is larger than the value,  $2\gamma$ , predicted by Griffith's theory.<sup>12</sup> For example, lattice trapping for (111) and (110) fracture in Si has been studied with electronic structure calculations based on the density functional theory (DFT).<sup>12</sup>

In the (111) brittle fracture, cleavagelike crack propagation occurs in a small range of  $G$  above  $G_c$ . At larger values of  $G$ , crack propagation becomes unstable against surface-step formation due to slip, as shown in Fig. 2(b). The slip plane observed in these simulations is  $\{11\bar{1}\}$ . This plane includes well-known shuffle and glide surfaces, and coincides with an experimentally observed easy slip plane.<sup>13</sup> The calculated  $G_c=4.6 \text{ J/m}^2$  is larger than  $2\gamma(111)=4.2 \text{ J/m}^2$ .

A snapshot of the (001) brittle fracture at  $G=9.5 \text{ J/m}^2$  is shown in Fig. 2(c). It is unstable against branching with {110} branched crack surfaces. The critical energy release rate,  $G_c(001)=5.1 \text{ J/m}^2$ , is close to  $\sqrt{2}G_c(110)$ , but smaller than  $2\gamma(001)=6.8 \text{ J/m}^2$ , which can be explained as the consequence of the branching along {110} surfaces. These features are akin to those obtained in our previous simulations in crystalline GaAs. Similar branching instabilities have been observed in MD simulations of various systems such as 2D triangular lattices,<sup>14,15</sup> Ni,<sup>16</sup> graphite,<sup>17</sup> and Si.<sup>18</sup>

The fracture toughness,  $T_c$ , is calculated as  $T_c=[G_c \times E/(1-\nu^2)]^{1/2}$ , where  $E$  is the Young's modulus and  $\nu$  is the Poisson ratio. The obtained fracture toughness,  $T_c$ , critical energy release rate,  $G_c$ , and surface energy,  $\gamma$ , are listed in Table I as well as available experimental and theoretical values. To our knowledge, no experimental data for single-crystal 3C-SiC are available. However, the surface energies are in reasonable agreement with other theoretical results.<sup>19-22</sup> The calculated critical energy release rates are in the range (3-7 J/m<sup>2</sup>), deduced by Rice *et al.*, from polycrystalline SiC.<sup>23</sup>

Figure 3 shows the crack-tip speed,  $\nu$ , as a function of  $G$  for the (110) fracture. The crack-tip speed rises sharply above  $G_c$ , and quickly saturates to a terminal speed (3720 m/s), which is about 53% of the Rayleigh wave speed (6963 m/s). This limiting speed is consistent with the results of previous MD simulations.<sup>3,4,14-18</sup> Above the critical energy release rate, crack propagation is observed in a wide range of  $G$ .

Figure 4 shows a snapshot of local stress distribution (tensile component) for (110) fracture at  $G=3.9 \text{ J/m}^2$ . Uni-

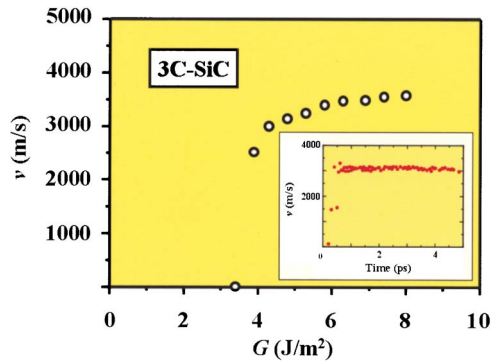


FIG. 3. Crack-tip speed,  $v$ , as a function of the mechanical release rate,  $G$ , for (110) dynamic fracture of 3C-SiC. The inset shows crack-tip speed as function of time at  $G=4.2$  J/m<sup>2</sup>.

form tensile stress extends in front of the crack tip, since the system is subjected to tension, whereas the stress is released immediately behind the tip due to new surface creation by the crack propagation. The estimated speed of the tensile-stress wave is about 12 000 m/s. It corresponds to the speed of longitudinal acoustic phonon along the  $[110]$  direction, which is 12 458 m/s. The figure also shows concentration of tensile stress around the crack tip as expected from elasticity theory. These stresses are monitored to check the boundary effects throughout the simulations. No significant perturbation due to those effects is observed in the stress field near the crack tip.

Dislocation activities at the crack tip have been studied extensively by MD simulations for metals such as Cu and Fe,<sup>24–26</sup> which in some cases result in extensive plasticity and make the fracture behaviors widely different from those reported here. To study the subtle competition between crack extension and dislocation emission, the interatomic potential needs to be carefully validated.<sup>6</sup>

Brittleness and ductility at the crack tip are dictated by the balance between the surface energy and the unstable stacking fault energy,  $\gamma_{\text{us}}$ , i.e., the energy barrier associated with a slip.<sup>27</sup> To validate our interatomic potential in this aspect, we have calculated  $\gamma_{\text{us}}$  for the (111) glide plane in the  $[10\bar{1}]$  direction with both MD and a quantum mechanical method in the framework of the density functional theory (DFT).<sup>28</sup> Following Tadmor and Hai,<sup>29</sup> the MD calculation starts with a bulk single-crystal sample with 21 atomic layers

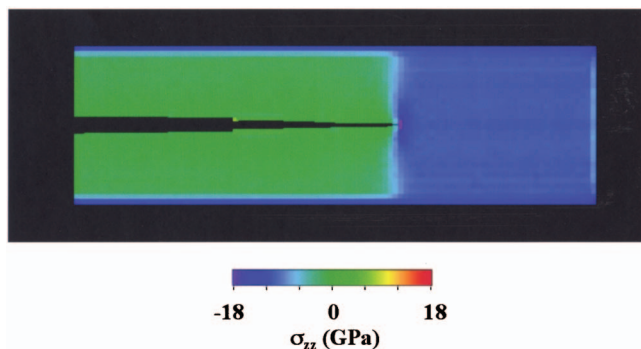


FIG. 4. (Color) A snapshot of local tensile-stress distribution in the (110) fracture simulation at  $G=3.9$  J/m<sup>2</sup>.

in the  $[111]$  direction. The top 10 layers are rigidly slid in the  $[10\bar{1}]$  direction against the bottom 11 layers, in several steps, forming an intrinsic stacking fault. The atomic positions in the  $[111]$  direction at each step are relaxed in order to obtain a minimum energy configuration. The electronic-structure calculations are based on the generalized gradient approximation<sup>30</sup> for the exchange-correlation energy in the DFT.<sup>31,32</sup> The ultrasoft pseudopotential<sup>33</sup> is employed to describe the interaction between the valence electrons and ions. The electronic wave functions and the electron density are expanded by the plane-wave basis sets with cutoff energies of 25 and 200 Ry, respectively. The energy functional is minimized using an iterative scheme based on a preconditioned conjugate-gradient method.<sup>34</sup> To calculate the DFT value for  $\gamma_{\text{us}}$ , we use a system consisting of 8 SiC layers with 10 Å vacuum, and relax the positions of atoms in the  $[111]$  direction. The stacking fault is created as stacking sequences, CABCABCA to CABCBCAB. The calculated MD value for the unstable stacking fault energy, 148 meV/Å<sup>2</sup>, agrees well with the DFT value, 169 meV/Å<sup>2</sup>. Our interatomic potential describes other mechanical properties of SiC as well. For example, the MD values for hardness agree well with experimental values.<sup>35</sup>

#### IV. SUMMARY AND DISCUSSION

In summary, molecular dynamics simulations have been carried out to investigate brittle fracture dynamics in crystalline 3C-SiC. The results show significant orientation dependence, that is (110) fracture is cleavage, whereas (111) and (001) fractures are unstable against slip and branching, respectively. Calculated critical energy release rates agree reasonably with the theoretical values, and support values predicted by Rice *et al.*

The present MD simulation results show a wide variety of fracture behaviors for different crystallographic planes. Previous theoretical studies have also shown that fracture could be highly anisotropic even within the same crack plane, i.e., cracks propagate differently for different crack propagation directions. For example, in the (110) plane in Si, a crack propagates in a cleavage manner in the  $\langle\bar{1}10\rangle$  direction, but it propagates discontinuously, with significant relaxation of the surrounding atoms, in the  $\langle 001\rangle$  direction.<sup>12</sup> Furthermore, full three-dimensional consideration of crack propagation brings in even more complex processes. For example, a recent theoretical study has shown a kink mechanism, in which the crack front propagates via formation of kinks, for (111) crack propagation in Si.<sup>36</sup>

#### ACKNOWLEDGMENTS

This work was supported by NSF, DOE, DARPA, and ARO. Simulations were performed using parallel computers at the Collaboratory of Advanced Computing and Simulations of the University of Southern California and at DoD Major Shared Resource Centers under a Challenge project. One of us (P.S.B.) acknowledges support from FAPESP (Fundação de Amparo à Pesquisa do Estado de São Paulo, SP-Brazil).

- <sup>1</sup>M. A. Capano and R. J. Trew, *MRS Bull.* **22**, 19 (1997).
- <sup>2</sup>J. Vashishta, R. K. Kalia, and A. Nakano, *Comput. Sci. Eng. Comput. Sci. Eng.* **1**, 56 (1999), and other articles in the same special issue on dynamic fracture.
- <sup>3</sup>D. Holland and M. Marder, *Phys. Rev. Lett.* **80**, 746 (1998).
- <sup>4</sup>J. Fineberg and M. Marder, *Phys. Rep.* **313**, 1 (1999).
- <sup>5</sup>J. Tersoff, *Phys. Rev. B* **39**, 5566 (1989).
- <sup>6</sup>C. Day, *Phys. Today* **52**(2), 17 (1999).
- <sup>7</sup>H. Kikuchi, R. K. Kalia, A. Nakano, and P. Vashishta (unpublished).
- <sup>8</sup>F. Shimojo, I. Ebbsjö, R. K. Kalia, A. Nakanol, J. P. Rino, and P. Vashishta, *Phys. Rev. Lett.* **84**, 3338 (2000).
- <sup>9</sup>A. Chatterjee, R. K. Kalia, C.-K. Loong, A. Nakano, A. Omeltchenko, K. Tsuruta, P. Vashishta, M. Winterer, and S. Klein, *Appl. Phys. Lett.* **77**, 1132 (2000).
- <sup>10</sup>J. P. Rino, I. Ebbsjö, P. S. Branicio, R. K. Kalia, A. Nakano, and P. Vashishta, *Phys. Rev. B* **70**, 045207 (2004).
- <sup>11</sup>B. Lawn, *Fracture of Brittle Solids* (Cambridge University Press, Cambridge, 1993).
- <sup>12</sup>R. Pérez and P. Gumbsch, *Acta Mater.* **48**, 4517 (2000).
- <sup>13</sup>A. George, *J. Phys. III* **1**, 909 (1991).
- <sup>14</sup>F. F. Abraham, D. Brodbeck, R. A. Rafey, and W. E. Rudge, *Phys. Rev. Lett.* **73**, 272 (1994).
- <sup>15</sup>S. J. Zhou, P. S. Lomdahl, R. Thomson, and B. L. Holian, *Phys. Rev. Lett.* **76**, 2318 (1996).
- <sup>16</sup>P. Gumbsch, S. J. Zhou, and B. L. Holian, *Phys. Rev. B* **55**, 3445 (1997).
- <sup>17</sup>A. Omeltchenko, J. Yu, R. K. Kalia, and P. Vashishta, *Phys. Rev. Lett.* **78**, 2148 (1997).
- <sup>18</sup>J. G. Swadener, M. I. Baskes, and M. Nastasi, *Phys. Rev. Lett.* **89**, 085503 (2002).
- <sup>19</sup>S. P. Mehandru and A. B. Anderson, *Phys. Rev. B* **42**, 9040 (1990).
- <sup>20</sup>D. H. Lee and J. D. Joannopoulos, *J. Vac. Sci. Technol.* **21**, 351 (1982).
- <sup>21</sup>T. Takai, T. Halicioglu, and W. A. Tiller, *Surf. Sci.* **164**, 341 (1985).
- <sup>22</sup>M. Tang and S. Yip, *Phys. Rev. B* **52**, 15150 (1995).
- <sup>23</sup>R. W. Rice, S. W. Freiman, R. C. Pohanka, J. J. Mecholsky, and C. C. Wu, in *Fracture Mechanics of Ceramics*, edited by R. C. Bradt, D. P. H. Haselmann, and F. F. Lange (Plenum, New York, 1978), Vol. 4, p. 840.
- <sup>24</sup>B. deCelis, A. S. Argon, and S. Yip, *J. Appl. Phys.* **54**, 4864 (1983).
- <sup>25</sup>S. J. Zhou, D. M. Beazley, P. S. Lomdahl, and B. L. Holian, *Phys. Rev. Lett.* **78**, 479 (1997).
- <sup>26</sup>T. Zhu, J. Li, and S. Yip, *Phys. Rev. Lett.* **93**, 025503 (2004).
- <sup>27</sup>J. R. Rice, *J. Mech. Phys. Solids* **40**, 239 (1992).
- <sup>28</sup>P. Hohenberg and W. Kohn, *Phys. Rev.* **136**, B864 (1964).
- <sup>29</sup>E. B. Tadmor and S. Hai, *J. Mech. Phys. Solids* **51**, 765 (2003).
- <sup>30</sup>J. P. Perdew, K. Burke, and M. Ernzerhof, *Phys. Rev. Lett.* **77**, 3865 (1996).
- <sup>31</sup>M. L. Cohen, *Science* **261**, 307 (1993).
- <sup>32</sup>F. Shimojo, R. K. Kalia, A. Nakano, and P. Vashishta, *Comput. Phys. Commun.* **140**, 303 (2001); **167**, 151 (2005).
- <sup>33</sup>D. Vanderbilt, *Phys. Rev. B* **41**, 7892 (1990).
- <sup>34</sup>G. Kresse and J. Hafner, *Phys. Rev. B* **49**, 14251 (1994).
- <sup>35</sup>I. Szlufarska, R. K. Kalia, A. Nakano, and P. Vashishta, *Appl. Phys. Lett.* **85**, 378 (2004); **86**, 021915 (2005); I. Szlufarska, A. Nakano, and P. Vashishta, *Science* **309**, 911 (2005).
- <sup>36</sup>T. Zhu, J. Li, and S. Yip, *Phys. Rev. Lett.* **93**, 205504 (2004).